

Research Article

Center-Vortex Loops with One Self-Intersection

Julian Moosmann and Ralf Hofmann

Institut für Theoretische Physik, Universität Karlsruhe (TH), Kaiserstrasse 12, 76131 Karlsruhe, Germany

Correspondence should be addressed to Ralf Hofmann, r.hofmann@thphys.uni-heidelberg.de

Received 7 December 2011; Accepted 1 April 2012

Academic Editors: E. Akhmedov and S. Ketov

Copyright © 2012 J. Moosmann and R. Hofmann. This is an open access article distributed under the Creative Commons Attribution License, which permits unrestricted use, distribution, and reproduction in any medium, provided the original work is properly cited.

We investigate the 2D behavior of one-fold self-intersecting, topologically stabilized center-vortex loops in the confining phase of an $SU(2)$ Yang-Mills theory. This coarse-graining is described by curve-shrinking evolution of center-vortex loops immersed in a flat 2D plane driving the renormalization-group flow of an effective “action.” We observe that the system evolves into a highly ordered state at finite noise level, and we speculate that this feature is connected with 2D planar high T_c superconductivity in FeAs systems.

1. Introduction

The idea of a nontrivial ground state being responsible for the emergence of “elementary” particles is a rather old one: already Lord Kelvin proposed that atoms and molecules should be considered knotted lines of vortices representing distortions in a universal medium (or ground state)—the ether [1]. As we know now, the physics of atoms and molecules described in terms of a much more efficient and elegant framework quantum mechanics. The agent responsible for the chemical bond—Lord Kelvin’s electron—is considered a spinning point particle in quantum mechanics, and this yields an excellent description of atomic physics, collider physics, and in the bulk of condensed matter physics.

There are, however, theoretical discrepancies with the concept of the electron being a point particle, and there are exceptional experimental situations pointing to the limitations of this concept to describe reality. As for the former, we have the old problem of a diverging classical self-energy not resolved in quantum electrodynamics where the electron mass is introduced as a free parameter whose running with resolution needs an experimental boundary condition. On the other hand, the two-dimensional dynamics of strongly correlated electrons in condensed matter physics signals the relevance of nonlocal effects possibly related to the nontrivial anatomy of the electron becoming relevant in collective phenomena

[2–4]. Also, recent high-temperature plasma experiments indicate unexpected explosive behavior not unlikely related to the mechanism for lepton emergence, see [5] and references therein.

Early papers, mostly investigating on a 4D Euclidean lattice the role of center vortices in forming a confining ground state at low temperatures/resolution [6–11], are based on the definition of a dual order parameter for quark confinement by [12]. Recent developments in understanding the confining phase of an SU(2) Yang-Mills theory suggest that Lord Kelvin’s ideas may actually be realized in Nature, see also [13–16]. The authors of [13–16] construct a plausible effective low-energy action for the 4D SU(2) Yang-Mills theory with solutions to the associated field equations representing closed confining strings knotted into stable solitons. In the thermodynamic approach of [17] the emergence of magnetic center-vortex loops (CVLs) is related to discontinuous phase changes of a complex order parameter for confinement across the (downward) Hagedorn transition and the fact that no magnetic charges exist where these flux lines could end. Also, it was discussed in [17] how the locations of topologically stabilized self-intersection represent isolated, spinning magnetic charges. (Notice that with respect to the electromagnetic U(1) of the Standard Model there is a dual interpretation of magnetic charges emerging in an SU(2) Yang-Mills theory).

In our previous article [18] we have investigated the sector with $N = 0$ self-intersections by considering a resolution-dependent ensemble average. The corresponding weight-functional is defined purely in terms of the planar curves’s geometry. The resolution dependence of this geometry, in turn, is determined by a curve-shrinking equation (heat-equation) [19, 20]. The validity of this description of spatial coarse-graining is motivated by considerations relating local curvature with the direction and speed of “motion” of the associated line-segment. The requirement that the partition function over a given ensemble of planar curves is invariant under a change of the resolution then yields the renormalization-group evolution of the weight-functional which is written as the exponential of an “action.” Here the term “action” is slightly misleading since we do not aim at describing the time-evolution of the system by demanding stationarity of the “action” under curve variation. To do the latter, a model, which relates resolution and time (being a macroscopic concept associated with the measuring apparatus), needs to be introduced. We thus regard resolution over time as the more fundamental quantity to describe certain subatomic systems. Our observation is that the effective “action” exhibits a transition towards dilational invariance after a finite, critical decrease of resolution. On average, CVLs with $N = 0$ are shrunk to circular points for a resolution less than the critical value which de facto removes them from the spectrum and thus generates an asymptotic mass gap. (CVLs with $N > 0$ are massive [17, 21]). Knowing the evolution of the weight-functional, one is in a position to compute the resolution dependence of “observables” as ensemble averages of the associated (nonlocal or local) “operators.” As for the evolution of the initially sharp center-of-mass position, we observe a spread of the variance with decreasing resolution saturating at a finite value. This is similar to the unitary free-particle evolution of a position eigenstate in quantum mechanics.

The purpose of the present paper is to extend the procedure of [18] to the case of $N = 1$. We now have a singled-out point on the curve: the location of the self-intersection where practically the entire mass of the soliton resides [17]. Setting the Yang-Mills scale Λ of the SU(2) theory equal to the electron mass $m_e = 511$ keV, which in turn determines the mass of the intersection point, we interpret this soliton as an electron or a positron [5, 21]. In the presence of a static electric or magnetic background field it is physically possible to lift the two-fold degeneracy w.r.t. the two possible directions of center-flux: the soliton exhibits a two-fold spin degeneracy. Notice that as long as both wings of center flux are of finite size

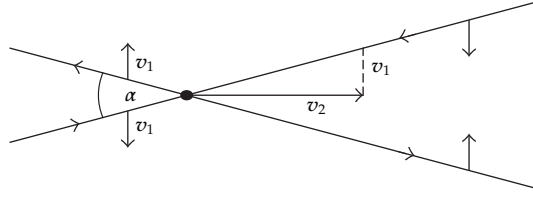


Figure 1: Points on the center flux lines moving oppositely on a line perpendicular to the bisecting line of the angle α with velocity modulus v_1 . For sufficiently small α the velocity modulus v_2 of the intersection point is superluminal: $v_2 = v_1 \cot(\alpha/2)$.

the position of the intersection point can be shifted at almost no cost of energy. In particular, if the inner angle α between in- and outgoing center-flux at the intersection is sufficiently small, then a motion of points on the vortex line directed perpendicular to the bisecting line of the angle α easily generates a velocity of the intersection point which exceeds the speed of light, see Figure 1. Recall that the path-integral formulation of quantum mechanics admits such superluminal motion in the sense that the according trajectories sizably contribute to transition amplitudes.

The paper is organized as follows. In Section 2 we discuss the physics associated with the emergence of topologically stabilized CVLs with intersection number $N = 1$, and how their spatial 2D coarse-graining is captured by a curve-shrinking flow. Some mathematical results on the properties of this flow for immersed curves, which are relevant for our subsequent numerical analysis, are briefly discussed. Also, we repeat our discussion in [18] of how the renormalization-group flow of an effective “action” is driven by the curve-shrinking evolution of the members of a given ensemble of curves. In Section 3 we explain our numerical analysis concerning the computation of the effective “action,” the variance of the location of the self-intersection, and the entropy associated with a given ensemble. Finally, in Section 4 we summarize our results and interpret them in view of certain 2D layered, quasimetallic systems exhibiting high- T_c superconductivity.

2. Conceptual Framework

2.1. Self-Intersecting Center-Vortex Loops

The transition from the non-self-intersecting to the self-intersecting CVL sector is by twisting of non-self-intersecting curves. The emergence of a localized (anti)monopole in the process is due to its capture by oppositely directed center fluxes in the intersection core (eye of the storm). By a rotation of the left half-plane in Figure 2(a) by an angle of π , see Figure 2(b), each wing of the CVLs forms a closed flux loop by itself thereby introducing equally directed center fluxes at the intersection point. This does not allow for an isolation of a single, spinning (anti)monopole in the core of the intersection and thus is topologically equivalent to the untwisted case Figure 2(a). However, another rotation of the left-most half-plane in Figure 2(c) introduces an intermediate loop which by shrinking is capable of isolating a spinning (anti)monopole due to oppositely directed center fluxes. Notice that in the last stage of such a shrinking process (short distances between the cores of the flux lines), propagating dual gauge modes are available. (On large distances these modes are infinitely massive which is characteristic of the confining phase): There is repulsion due to Biot-Savart which needs to

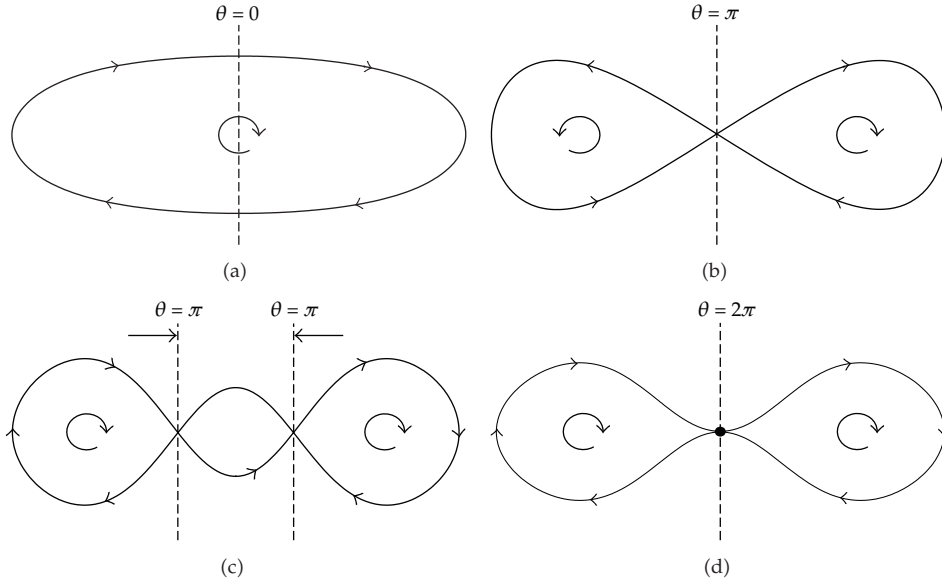


Figure 2: (Topological) transition from the $N = 0$ sector (a), (b), (c) to the $N = 1$ sector (d) by twisting and subsequent capture of a magnetic (anti)monopole in the core of the final intersection. Arrows indicate the direction of center flux.

be overcome. This necessitates an investment of energy manifesting itself in terms of the mass of the isolated (anti)monopole (eye of the storm). Alternatively, the emergence of an isolated (anti)monopole is possible by a simple pinching of the untwisted curve, again having to overcome local repulsion in the final stage of this process.

For the analysis performed in the present work we solely regard the situation depicted in Figure 2(d) and thus no longer need to discuss the direction of center flux within a given curve segment. This is not relevant for the process of a spatial coarse-graining microscopically described by the same curve-shrinking flow as applied to sector with $N = 0$ [18].

2.2. Euclidean Curve Shrinking Flow

The restriction of evolution of a CVL with self-intersection number $N = 1$ to the plane is an essential constraint on generality if we aim at a fundamental description of the effectively quantum mechanical behavior of a charged lepton (electron, muon, tau-lepton). An electron bound inside a hydrogen atom certainly “moves” in 3D and quantum mechanics describing it as a spinning, relativistic point particle is in accurate agreement with experiment. The quantum mechanically incompletely understood condensed-matter physics of strongly correlated 2D electrons, however, is a possibly fertile application field of our restriction of curve evolution to the plane, see Section 4.

Notice that by immersing an $SU(2)$ CVL with finite core size d and mass m_D of the dual gauge field into a flat 2D surface at $m_D < \infty$, $d > 0$, a hypothetic observer measuring a positive (negative) curvature of a segment of the vortex line experiences more (less) negative pressure in the intermediate vicinity of this curve segment leading to its motion towards (away from) the observer, see Figure 3.

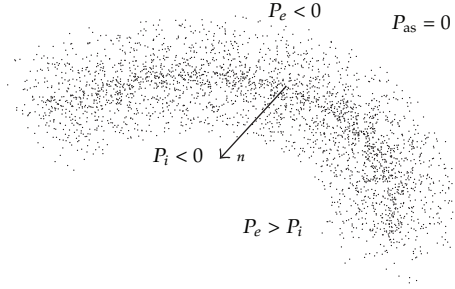


Figure 3: Highly space-resolved snapshot of a CVL segment. The pressure P_i in the region pointed to by the normal vector \mathbf{n} is more negative than the pressure P_e thus leading to a motion of the segment along \mathbf{n} .

The (inward directed) speed of a point in the core of the vortex will be a monotonic function of the curvature at this point. On average, this shrinks the CVL. Alternatively, one may *globally* consider the limit $m_D \rightarrow \infty$, $d \rightarrow 0$, that is, the confining phase of an $SU(2)$ Yang-Mills theory, but now take into account the effects of an environment which *locally* relaxes this limit (by collisions) and thus also induces curve shrinking. This situation is described by the following equation for a flow in the (dimensionless) parameter τ :

$$\partial_\tau \mathbf{x} = \frac{1}{\sigma} \partial_s^2 \mathbf{x}, \quad (2.1)$$

where s is arc length, \mathbf{x} is a point on the CVL in the plane, and σ is a string tension effectively expressing the distortions induced by the environment. After a rescaling, $\hat{\mathbf{x}} \equiv \sqrt{\sigma} \mathbf{x}$, $\xi = \sqrt{\sigma} s$, (2.1) assumes the following form

$$\partial_\tau \hat{\mathbf{x}}(u, \tau) = \partial_\xi^2 \hat{\mathbf{x}} = k(u, \tau) \mathbf{n}(u, \tau), \quad (2.2)$$

where u is a (dimensionless) curve parameter, \mathbf{n} the (inward-pointing) Euclidean unit normal, k the scalar curvature, defined as

$$k \equiv \left| \partial_\xi^2 \hat{\mathbf{x}} \right| = \left| \frac{1}{|\partial_u \hat{\mathbf{x}}|} \partial_u \left(\frac{1}{|\partial_u \hat{\mathbf{x}}|} \partial_u \hat{\mathbf{x}} \right) \right|, \quad (2.3)$$

$|\mathbf{v}| \equiv \sqrt{\mathbf{v} \cdot \mathbf{v}}$, and $\mathbf{v} \cdot \mathbf{w}$ denotes the Euclidean scalar product of the vectors \mathbf{v} and \mathbf{w} . In the following we resort to a slight abuse of notation by using the same symbol $\hat{\mathbf{x}}$ for the functional dependence on u or ξ .

We now consider curves with one self-intersection, that is, $N = 1$, in the sense of the stable situation of Figure 2(d). This situation was mathematically analysed in [22]. Since the direction of center flux is inessential for the shrinking process we may actually treat this situation in a way as depicted in Figure 2(b), where the curve is defined to be a smooth immersion into the plane with exactly one double point and a total rotation number zero, $\int_0^L k d\xi = 0$. Here the (dimensionless) curve length L is given by the smooth integration $L(\tau) = \int_0^{L(\tau)} d\xi = \int_0^{2\pi} du |\partial_u \hat{\mathbf{x}}(u, \tau)|$. Notice that this is topologically distinct from the case Figure 2(d) where one encounters a nonvanishing rotation number which is not smoothly deformable to zero.

In the $N = 0$ case a smooth, embedded curve shrinks to a circular point under the flow for $\tau \nearrow T < \infty$ [19, 20]. That is, the isoperimetric ratio approaches 4π from above. The curve in situation Figure 2(b) separates the plane into three disjoint areas two of which are finite and denoted by A_1 and A_2 . We understand by T the finite, critical value of τ where either A_1 or A_2 or both vanish. This corresponds to a singularity encountered and thus terminates the flow.

Recall that in the $N = 0$ case the rate of area change is a constant, $dA/d\tau = -2\pi$. This is no longer true for $N = 1$. However, we have that

$$A_1(\tau) - A_2(\tau) = \text{const.} \quad (2.4)$$

Also, for $N = 1$ we have in comparison to the $N = 0$ case the more relaxed constraint that $-4\pi \leq d(A_1 + A_2)/d\tau \leq -2\pi$.

In contrast to the $N = 0$ case the isoperimetric ratio for the $N = 1$ case is bounded for $\tau \nearrow T$ if and only if $A_1 \neq A_2$. Notice that the case $A_1 = A_2$ physically is extremely fine-tuned.

2.3. Effective “Action”

We now wish to interpret curve-shrinking as a Wilsonian renormalization-group flow taking place in the $N = 1$ CVL sector in the sense defined in Section 2.2. A partition function, defined as a statistical average (according to a suitably defined weight) over $N = 1$ CVLs, is to be left invariant under a decrease of the resolution determined by the flow parameter τ . Notice that, physically, τ is interpreted as a strictly monotonic decreasing (dimensionless) function of a ratio Q/Q_0 where Q (Q_0) are mass scales associated with an actual (initial) resolution applied to the system. The role of Q can also be played by the finite temperature of a reservoir coupled to the system.

To devise a geometric ansatz for the effective “action” $S = S[\hat{x}(\tau)]$, which is a functional of the curve \hat{x} representable in terms of integrals over local densities in ξ (reparametrization invariance), the following reflection on symmetries is in order. (i) Scaling symmetry $\hat{x} \rightarrow \lambda\hat{x}$, $\lambda \in \mathbf{R}_+$: for $\lambda \rightarrow \infty$, implying $\lambda L \rightarrow \infty$ at fixed L , the “action” S should be invariant under further finite rescalings (decoupling of the fixed length scales $\sigma^{-1/2}$ and Λ^{-1}), (ii) Euclidean point symmetry of the plane (rotations, translations, and reflections about a given axis): Sufficient but not necessary for this is a representation of S in terms of integrals over scalar densities w.r.t. these symmetries. That is, the “action” density should be expressible as a series involving products of Euclidean scalar products of $(\partial^n/\partial\xi^n)\hat{x}$, $n \in \mathbf{N}_+$, or constancy. However, an exceptional scalar integral over a nonscalar density can be devised. Consider the area A , calculated as

$$A = \left| \frac{1}{2} \int_0^{2\pi} d\xi \hat{x} \cdot \mathbf{n} \right|. \quad (2.5)$$

The density $\hat{x} \cdot \mathbf{n}$ in (2.5) is not a scalar under translations.

We now resort to a factorization ansatz as

$$S = F_c \times F_{nc}, \quad (2.6)$$

where in addition to Euclidean point symmetry F_c (F_{nc}) is (is not) invariant under $\hat{x} \rightarrow \lambda\hat{x}$. In principle, infinitely many operators can be defined to contribute to F_c . Since the

evolution homogenizes the curvature except for a small vicinity of the intersection point higher derivatives of k w.r.t. ξ should not be of importance. We expect this to be true also for Euclidean scalar products involving higher derivatives $(\partial^n/\partial\xi^n)\hat{x}$. To yield conformally invariant expressions such integrals need to be multiplied by powers of \sqrt{A} and/or L or the inverse of integrals involving lower derivatives. At this stage, we are not capable of constraining the expansion in derivatives by additional physical or mathematical arguments. To be pragmatic, we simply set F_c equal to the isoperimetric ratio:

$$F_c(\tau) \equiv \frac{L(\tau)^2}{A(\tau)}. \quad (2.7)$$

We conceive the nonconformal factor F_{nc} in S as a formal Taylor expansion in inverse powers of L or $A \equiv A_1 + A_2$ due to the property of conformal invariance for $L, A \rightarrow \infty$.

Since we regard the renormalization-group evolution of the effective “action” as induced by the flow of an ensemble of curves, where the evolution of each member is dictated by (2.2), we allow for an explicit τ dependence of the coefficient c of the lowest nontrivial power $1/L$ or $1/A$. In principle, this sums up the contribution to F_{nc} of certain higher-power operators which do not exhibit an explicit τ dependence. Hence we make the following ansatz:

$$F_{nc}(\tau) = 1 + \frac{c(\tau)}{L(\tau)}. \quad (2.8)$$

The initial value $c(\tau = 0)$ is determined from a physical boundary condition such as the mean length \bar{L} at $\tau = 0$.

2.4. Geometric Partition Function

Let us now numerically investigate the effective “action” $S[\hat{x}(\tau)]$ resulting from a partition function Z w.r.t. a nontrivial ensemble E . The latter is defined as the average

$$Z = \sum_i \exp(-S[\hat{x}_i(\tau)]) \quad (2.9)$$

over the ensemble $E = \{\hat{x}_1, \dots\}$. Let us denote by E_M an ensemble consisting of M curves where E_M is obtained from E_{M-1} by adding a new curve $\hat{x}_M(u, \tau)$. The effective “action” S in (2.6) (when associated with the ensemble E_M we will denote it by S_M) is determined by the function $c_M(\tau)$, compare with (2.8), whose flow follows from the requirement of τ -independence of Z_M :

$$\frac{d}{d\tau} Z_M = 0. \quad (2.10)$$

This is an implicit, first-order ordinary differential equation for $c(\tau)$ which needs to be supplemented with an initial condition $c_{0,M} = c_M(\tau = 0)$. A natural initial condition is to demand that the quantity

$$\bar{L}_M(\tau = 0) \equiv \frac{1}{Z_M(\tau = 0)} \sum_{i=1}^M L[\hat{x}_i(\tau = 0)] \exp(-S_M[\hat{x}_i(\tau = 0)]) \quad (2.11)$$

coincides with the algebraic mean $\tilde{L}_M(\tau = 0)$ defined as

$$\tilde{L}_M(\tau = 0) \equiv \frac{1}{M} \sum_{i=1}^M L[\hat{x}_i(\tau = 0)]. \quad (2.12)$$

From $\bar{L}_M(\tau = 0) = \tilde{L}_M(\tau = 0)$ a value for $c_{0,M}$ follows. We also have considered a modified factor

$$F_{nc}(\tau) = 1 + \frac{c(\tau)}{A(\tau)}. \quad (2.13)$$

While, due to (2.13), the ansatz for the geometric effective "action" in (2.6) thus is profoundly different for such a modification of $F_{nc}(\tau)$ physical results such as the evolution of the variance of the intersection agree remarkably well, see Section 3.

3. Results of Simulation

3.1. Preparation of Ensembles

Similar as in [18] we normalize all curves to have the same initial area $A_0 = A_{0,1} + A_{0,2}$, and, since we are now interested in the position of the intersection where the (anti)monopole, is localized, we have applied a translation to each curves in the ensembles E_M such that the location of the intersections initially coincides with the origin.

Since the critical value T of the flow parameter τ varies from curve to curve, we order the members of the maximal-size ensemble $E_{M=16}$ into subensembles $E_{M<16}$ such that $T_{i=1} \geq T_{i=2} \geq \dots \geq T_M$. The types of ensembles E_M obtained in this way are referred to as T -ordered. We also have performed all simulations with ensembles $E'_{M<16}$ whose members are picked randomly from $E_{M=16}$ and have obtained strikingly similar results for ensemble averages of "observables" using $E_{M<16}$ and $E'_{M<16}$ for the τ evolution to the left of $\tau = \min\{T_i \mid \hat{x}_i \in E'_{M<16}\}$.

The maximal-size ensemble $E_{M=16}$ at $\tau = 0$ is depicted in Figure 4 with the universal choice $A_0 = 200\pi$. The curves in Figure 4 are arranged in a T -ordered way. We have $T_{i=1} = 65 \geq T_{i=2} \geq \dots \geq T_M = 43$. In Figure 5 the evolution of an initial curve under curve shrinking is shown from two viewpoints. The flow is started at $\tau = 0$ and stopped at a value of τ shortly below T . In Figure 6 the flow of the intersection points, corresponding to the initial curves depicted in Figure 4, is shown. The search for solutions to the second-order partial differential equation (PDE) (2.2) subject to periodic boundary conditions in the curve parameter, $\hat{x}(u = 0, \tau = 0) = \hat{x}(u = 2\pi, \tau = 0)$, and for the initial conditions $\hat{x}(u, \tau = 0)$ depicted in Figure 4

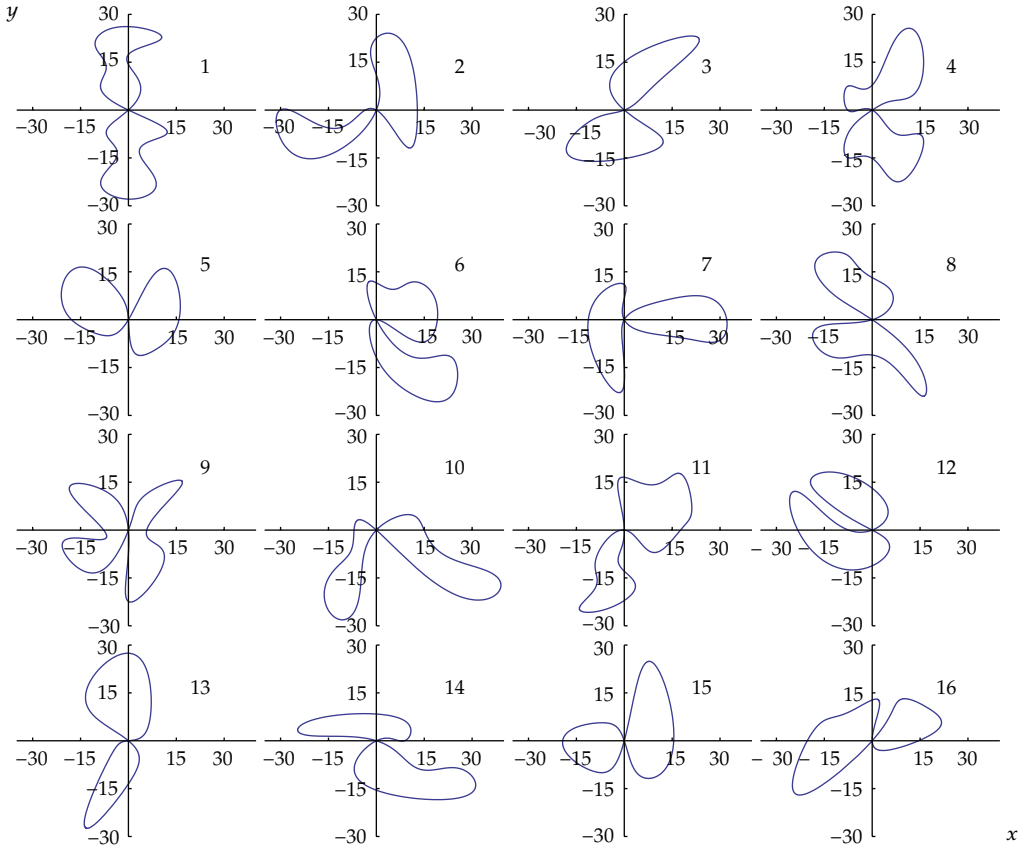


Figure 4: Initial curves $\hat{x}_i(u, \tau = 0)$ contributing to the ensemble $E_{M=16}$. The intersection points coincide with the origin, and all curves have the same area 200π . By definition $E_{M=16}$ is T -ordered.

was performed numerically using the method of lines. That is, the PDE was discretized on a uniform grid in the parameter u yielding a semidiscrete problem in terms of a system of ordinary differential equations (ODEs) in τ which was solved using Mathematica. Figure 5 indicates why this technique is called the numerical method of lines. As one can also see from Figure 5, a set of discrete points on the curve, although remaining equidistant in u , may evolve under the flow such that the spatial distances between next-neighbours-points fall below the numerical precision. Numerically, the flow then encounters a singularity (not to confused with the earlier mentioned nonfictitious singularities). To recognize such a situation automatically, (2.4) was exploited: the evolution was stopped as soon as a sizable deviation occurred from what (2.4) predicts. The configuration obtained at this point in τ was fitted in such a way that a new discretization in u yielded well-separated points to restart the methods of lines. (2.4) was also used as an indicator for the final singularity at T where A_1 or A_2 or both vanish.

3.2. Renormalization-Group Invariance of Partition Function

For all ensembles E_M , the τ dependence of the coefficient c_M in (2.8) roughly behaves like a square root $\propto \sqrt{T_M - \tau}$, where T_M is the weakly ensemble-dependent minimal resolution.

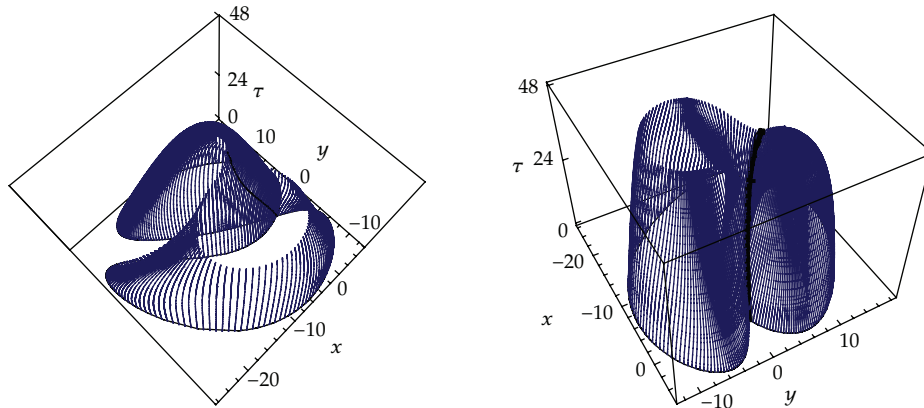


Figure 5: Plot of the evolution of an $N = 1$ CVL (curve 12 of Figure 4) under (2.2). The thick central line indicates the trajectory of the intersection point which coincides with the origin at $\tau = 0$.

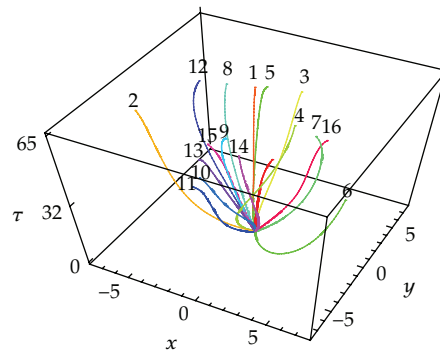


Figure 6: Flow of the intersection points for the initial curves depicted in Figure 4.

For the modified “action” $S_M = (L(t)^2/A(t))(1 + (c_M(t)/A(t)))$ the coefficient c_M is well approximated by a linear function $\propto T_M - \tau$. Again, T_M denotes a weakly ensemble-dependent minimal resolution. For T -ordered ensembles, the results for c_M for the “actions” (2.8) and (2.13) are shown in Figures 7 and 8, respectively. The results for ensembles E'_M do not differ sizably from those presented in Figures 7 and 8.

3.3. Variance of Location of Self-Intersection

The mean intersection $\overline{\hat{x}_{\text{int}}}$ over the ensemble E_M is defined as

$$\overline{\hat{x}_{\text{int}}}(\tau) \equiv \frac{1}{Z_M} \sum_{i=1}^M \hat{x}_{\text{int},i}(\tau) \exp(-S_M[\hat{x}_i(\tau)]), \quad (3.1)$$

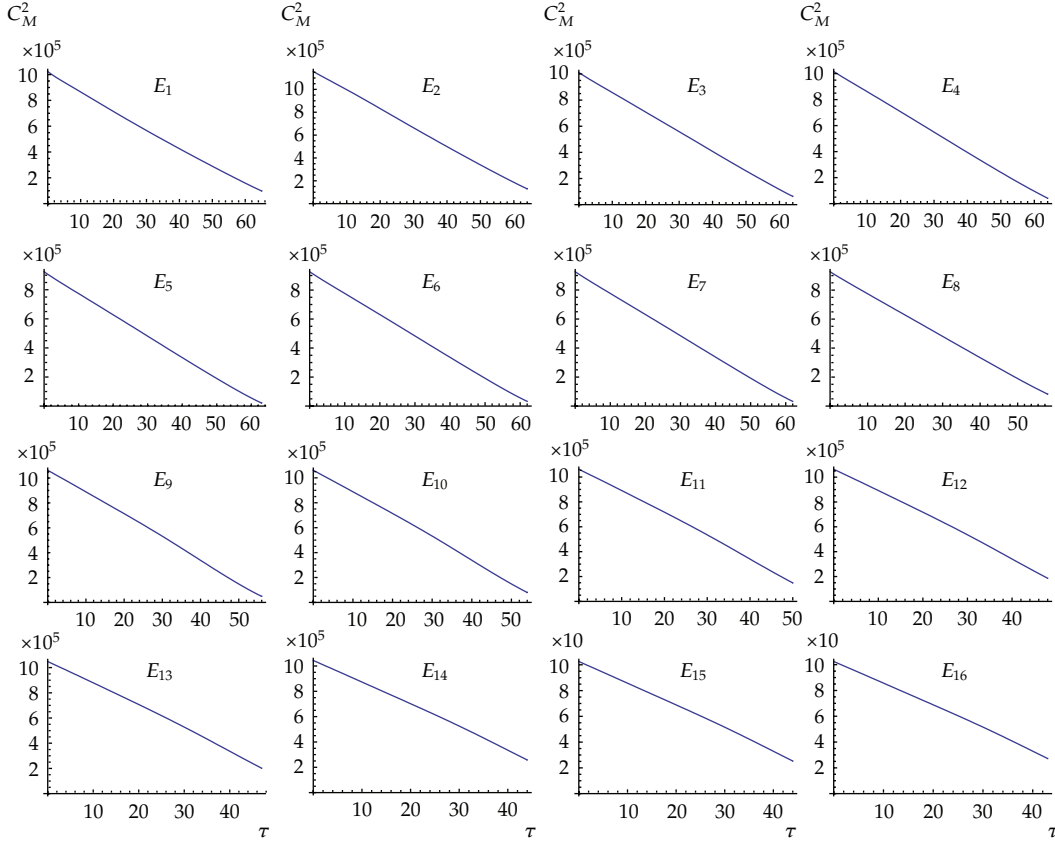


Figure 7: The squares of the coefficients $c_M(\tau)$ entering the ansatz for effective “action” of (2.6) specializing to (2.8) for T -ordered ensembles up to $M = 16$.

where $\hat{x}_{\text{int},i}(\tau)$ is the location of self-intersection (intersection point) of curve \hat{x}_i at τ . The scalar statistical deviation $\Delta_{M,\text{int}}$ of $\bar{\hat{x}}_{\text{int}}$ over the ensemble E_M is defined as

$$\Delta_{M,\text{int}}(\tau) \equiv \sqrt{\text{var}_{M,\text{int},x}(\tau) + \text{var}_{M,\text{int},y}(\tau)}, \quad (3.2)$$

where

$$\begin{aligned} \text{var}_{M,\text{int},x} &\equiv \frac{1}{Z_M} \sum_{i=1}^M (x_{\text{int},i}(\tau) - \bar{x}_{\text{int}}(\tau))^2 \exp(-S_M[\hat{x}_i(\tau)]) \\ &= -\bar{x}_{\text{int}}^2(\tau) + \frac{1}{Z_M} \sum_{i=1}^M x_{\text{int},i}^2(\tau) \exp(-S_M[\hat{x}_i(\tau)]) \end{aligned} \quad (3.3)$$

and similarly for the coordinate y . In Figure 9 plots of $\Delta_{M,\text{int}}(\tau)$ are shown when evaluated over the ensembles E_1, \dots, E_{16} subject to the “action”

$$S_M = \frac{L(\tau)^2}{A(\tau)} \left(1 + \frac{c_M(\tau)}{L(\tau)} \right) \quad (3.4)$$

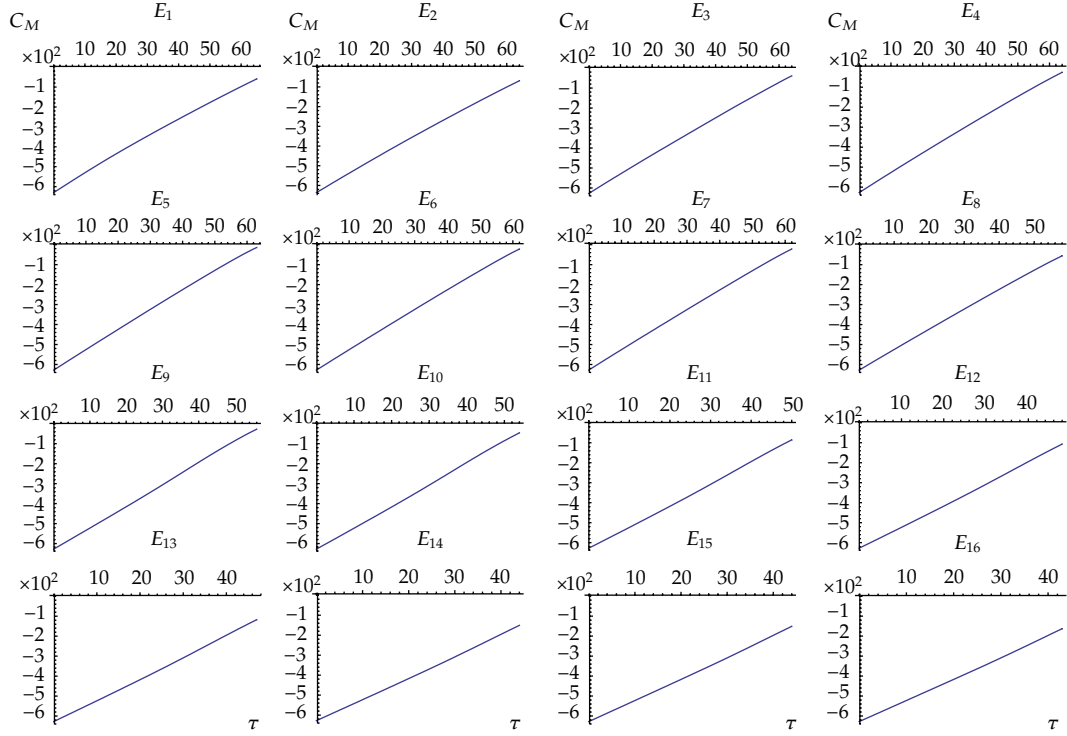


Figure 8: The coefficient $c_M(\tau)$ entering the ansatz for the effective “action” of (2.6) specializing to (2.13) for T -ordered ensembles up to $M = 16$.

and the initial condition $\bar{L}_M(\tau = 0) = \tilde{L}_M(\tau = 0)$. In Figure 10 the according plots of $\Delta_{M,\text{int}}(\tau)$ are depicted as obtained with the “action”

$$S_M = \frac{L(\tau)^2}{A(\tau)} \left(1 + \frac{c_M(\tau)}{A(\tau)} \right) \quad (3.5)$$

and subject to the initial condition $\bar{L}_M(\tau = 0) = \tilde{L}_M(\tau = 0)$. Relaxing the constraint of T -ordering ($E_M \rightarrow E'_M$) does not entail a qualitative change of the results.

The results presented in Figures 9 and 10 are unexpected since in the $N = 0$ sector the variance of the “center-of-mass” saturates rapidly to finite values. In contrast, for the $N = 1$ sector the variance of the location of the self-intersection initially increases, reaches a maximum, and decreases to zero at a *finite* value of τ . This is readily confirmed by the evaluation of the entropy, see Section 3.4.

3.4. Evolution of Entropy

Let us now evaluate the flow of entropy Σ_M defined as

$$\Sigma_M(\tau) \equiv \log Z_M + \frac{1}{Z_M} \sum_{i=1}^M \exp(-S_M[\hat{x}_i(\tau)]) S_M[\hat{x}_i(\tau)], \quad (3.6)$$

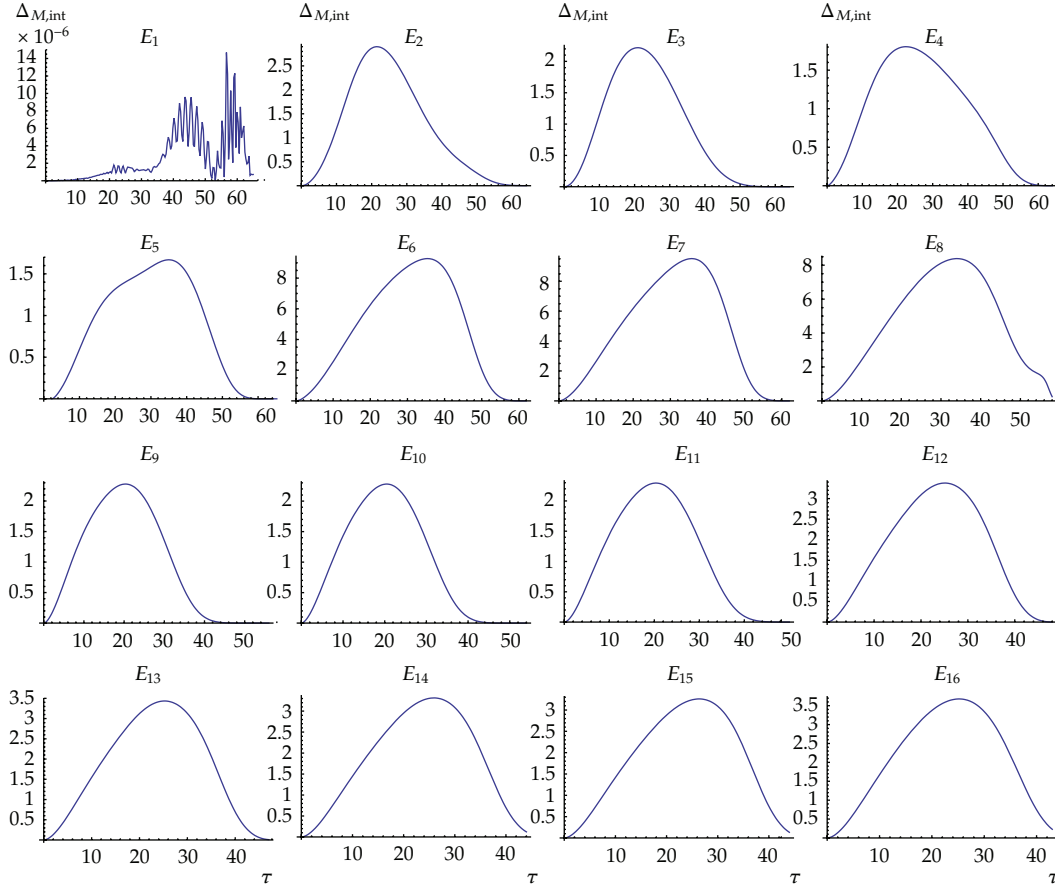


Figure 9: Plots of $\Delta_{M,\text{int}}(\tau)$ for the T -ordered ensembles E_M with $M = 1, \dots, 16$. We have employed the ansatz for the “action” $S_M = (L(\tau)^2/A(\tau))(1 + (c_M(\tau)/L(\tau)))$.

where $S_M[\hat{x}_i(\tau)]$ is given by (2.6). In Figure 11 plots are shown for $\Sigma_M(\tau)$. when evaluated with the “action” $S_M = (L(\tau)^2/A(\tau))(1 + (c_M(\tau)/L(\tau)))$ for T -ordered ensembles of size $M = 1, \dots, 16$. These graphs look very much alike to the ones generated using the “action” $S_M = (L(\tau)^2/A(\tau))(1 + (c_M(\tau)/A(\tau)))$. Notice the continuous approach to zero at finite values of τ . This implies that order emerges spontaneously in the system with decreasing resolution: starting at a finite value of τ , a particular member of E_M is singled out by its weight approaching unity. Judging from our results for the $N = 0$ sector [18], this behavior is highly unexpected. Therefore the nontrivial topology of $N = 1$ induces qualitative differences to the coarse-graining process.

4. Summary, Interpretation of Results, and Conclusion

In this paper we have investigated the spatial coarse-graining of CVLs, immersed in a flat 2D plane, of an $SU(2)$ Yang-Mills theory being in its confining phase. The focus was on the sector with one topologically stabilized self-intersection (existence of an isolated magnetic charge at its location, $N = 1$). We have analysed this coarse-graining process in terms

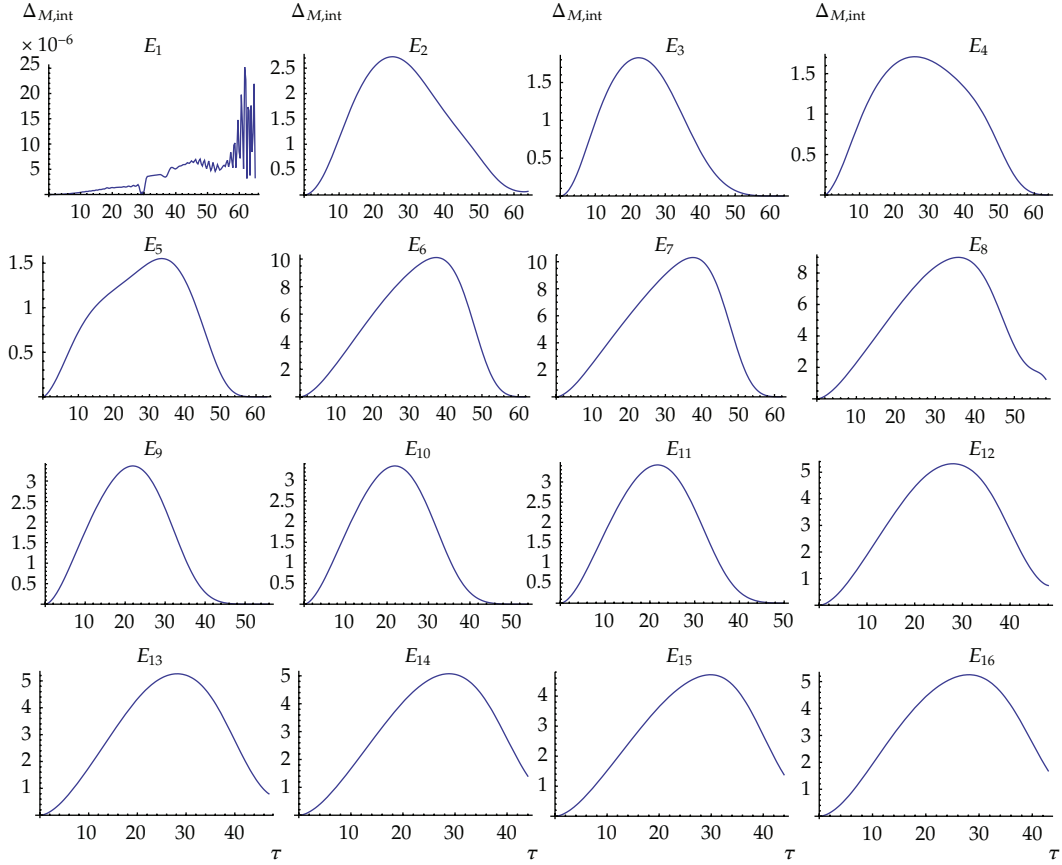


Figure 10: Plots of $\Delta_{M,int}(\tau)$ for the T -ordered ensembles E_M with $M = 1, \dots, 16$. We have employed the ansatz for the “action” $S_M = (L(\tau)^2/A(\tau))(1 + (c_M(\tau)/A(\tau)))$.

of curve ensembles generated by evolving an initial situation under the curve-shrinking flow [19, 20, 22]. The idea here is to suppose that curve shrinking in the parameter τ represents an exact coarse-graining of a given initial state and to reconstruct the associated ensemble-weight of the statistical approach (exponential of effective “action”) by demanding invariance of the corresponding partition function under the flow in τ (renormalization-group evolution). Notice that τ is related to a physical resolution, applied to probing the system, in a strictly monotonic decreasing manner. This resolution may be associated with a local momentum transfer exerted by an observer or a globally defined temperature of an environment. The functional dependence of τ on these physical parameters depends on the given experimental situation. It is, however, reasonable to assume that *finite* values of τ universally correspond to *finite* values of these physical parameters.

In Sections 3.3 and 3.4 we have obtained the unexpected result that a statistical ensemble of renormalization-group evolved curves spontaneously orders itself in the sense that, starting from finite values of τ , only a particular member of the ensemble survives the process of 2D spatial coarse-graining. That is, the entropy attributed to the ensemble is practically zero for sufficiently large values of τ . For the location of self-intersection (charge of an electron) this means that no dissipation of energy, provided by the environment, can be

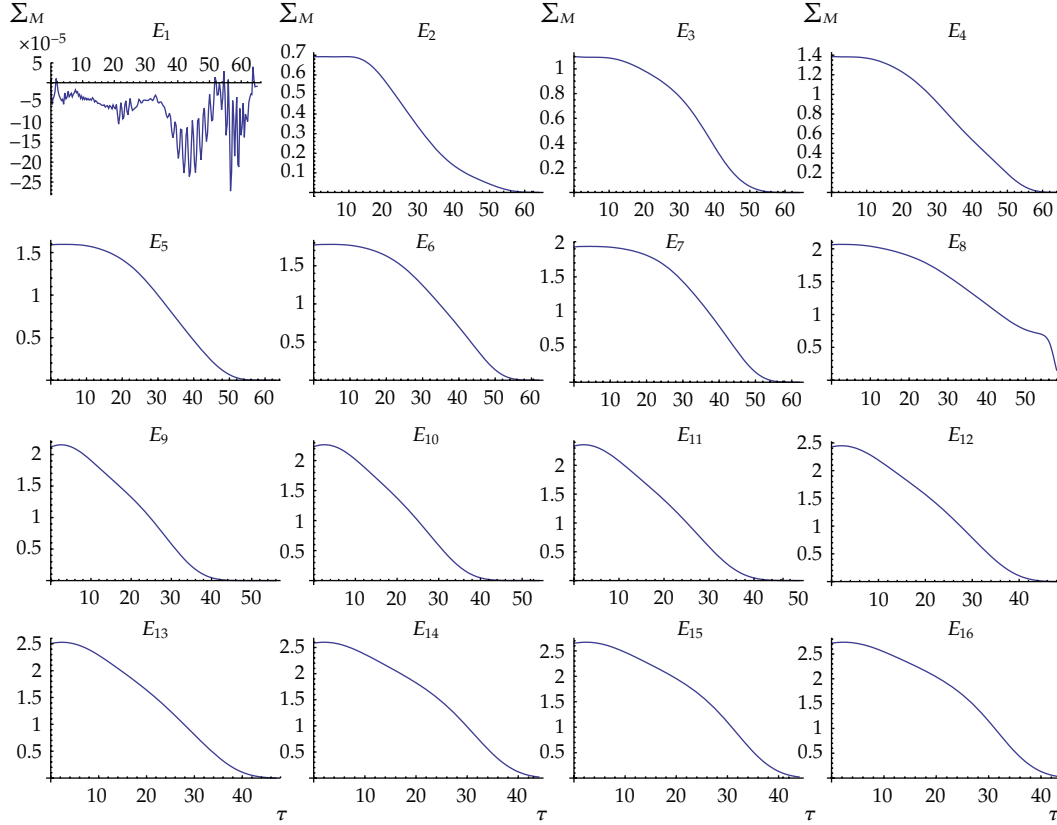


Figure 11: Flow of the entropies Σ_M for T -ordered ensembles of size $M = 1, \dots, 16$ when evaluated with the “action” $S_M = (L(\tau)^2/A(\tau))(1 + (c_M(\tau)/L(\tau)))$. The situation does not change qualitatively if the “action” $S_M = (L(\tau)^2/A(\tau))(1 + (c_M(\tau)/A(\tau)))$ is used.

mediated by the monopole situated within the core of the intersection if the resolution falls below a critical, *finite* value. This result must drastically depend on the two-dimensionality of space and the fact that we consider the sector with $N = 1$, compare with [18].

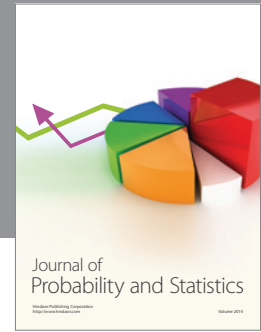
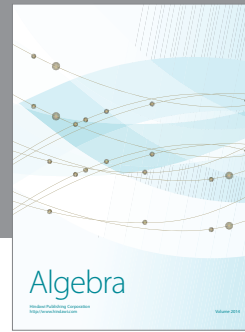
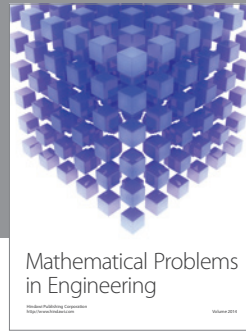
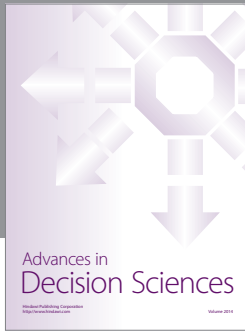
The recently discovered, unconventional FeAs systems do not appear to exhibit an explicit, strong correlation between the electrons contained in their theoretically suggested, 2D-superconducting layers, see [23] and references therein. If the two-dimensional behavior of noninteracting electrons, subject to an environment represented by the parameter τ , indeed is described by the coarse-graining process investigated in the present work, then the sudden decrease of entropy that we observe at a *finite* value of τ should ultimately be connected to this particular kind of high- T_c superconductivity. Here τ is a monotonically decreasing function of temperature.

Acknowledgment

The authors would like to thank Francesco Giacosa and Markus Schwarz for useful conversations.

References

- [1] W. T. Kelvin and P. G. Tait, *Treatise on Natural Philosophy*, vol. 2, Cambridge University Press, 1867.
- [2] J. G. Bednorz and K. A. Müller, "Possible high T_c superconductivity in the Ba-La-Cu-O system," *Zeitschrift für Physik B Condensed Matter*, vol. 64, no. 2, pp. 189–193, 1986.
- [3] P. W. Anderson, "Present status of the theory of high T_c cuprates," <http://arxiv.org/abs/cond-mat/0510053>.
- [4] P. W. Anderson, "Twenty years of talking past each other: the theory of high T_c ," *Physica C*, vol. 460–462, pp. 3–6, 2007.
- [5] F. Giacosa, R. Hofmann, and M. Schwarz, "Explosive Z pinch," *Modern Physics Letters A*, vol. 21, no. 36, pp. 2709–2715, 2006.
- [6] G. Mack and V. B. Petkova, "Comparison of lattice gauge theories with gauge groups Z_2 and $SU(2)$," *Annals of Physics*, vol. 123, no. 2, pp. 442–467, 1979.
- [7] G. Mack, "Predictions of a theory of quark confinement," *Physical Review Letters*, vol. 45, no. 17, pp. 1378–1381, 1980.
- [8] G. Mack and V. B. Petkova, "Sufficient condition for confinement of static quarks by a vortex condensation mechanism," *Annals of Physics*, vol. 125, no. 1, pp. 117–134, 1980.
- [9] G. Mack and E. Pietarinen, "Monopoles, vortices and confinement," *Nuclear Physics B*, vol. 205, no. 2, pp. 141–167, 1982.
- [10] H. B. Nielsen and P. Olesen, "A quantum liquid model for the QCD vacuum. Gauge and rotational invariance of domained and quantized homogeneous color fields," *Nuclear Physics B*, vol. 160, no. 2, pp. 380–396, 1979.
- [11] E. Tomboulis, "'t Hooft loop in $SU(2)$ lattice gauge theories," *Physical Review D*, vol. 23, no. 10, pp. 2371–2383, 1981.
- [12] G. 't Hooft, "On the phase transition towards permanent quark confinement," *Nuclear Physics B*, vol. 138, no. 1, pp. 1–25, 1978.
- [13] L. Faddeev and Antti J. Niemi, "Stable knot-like structures in classical field theory," *Nature*, vol. 387, no. 6628, pp. 58–61, 1997.
- [14] L. Faddeev and A. J. Niemi, "Partially dual variables in $SU(2)$ Yang-Mills theory," *Physical Review Letters*, vol. 82, no. 8, pp. 1624–1627, 1999.
- [15] L. Faddeev and A. J. Niemi, "Aspects of electric and magnetic variables in $SU(2)$ Yang-Mills theory," *Physics Letters. B*, vol. 525, no. 1–2, pp. 195–200, 2002.
- [16] L. Faddeev and A. J. Niemi, "Spin-charge separation, conformal covariance and the $SU(2)$ Yang-Mills theory," *Nuclear Physics B*, vol. 776, no. 1–2, pp. 38–65, 2007.
- [17] R. Hofmann, "Nonperturbative approach to Yang-Mills thermodynamics," *International Journal of Modern Physics A*, vol. 20, no. 18, pp. 4123–4216, 2005, Erratum vol. 21, pp. 6515–6523, 2006.
- [18] J. Moosmann and R. Hofmann, "Evolving center-vortex loops," <http://arxiv.org/abs/0804.3527>.
- [19] M. Gage and R. S. Hamilton, "The heat equation shrinking convex plane curves," *Journal of Differential Geometry*, vol. 23, no. 1, pp. 69–96, 1986.
- [20] M. A. Grayson, "The heat equation shrinks embedded plane curves to round points," *Journal of Differential Geometry*, vol. 26, no. 2, pp. 285–314, 1987.
- [21] R. Hofmann, "Yang-Mills thermodynamics," <http://arxiv.org/abs/0710.0962>.
- [22] M. A. Grayson, "The shape of a figure-eight under the curve shortening flow," *Inventiones Mathematicae*, vol. 96, no. 1, pp. 177–180, 1989.
- [23] H.-H. Klauss and B. Büchner, "Neuer Goldrausch in der Supraleitung," *Physik Journal*, vol. 7, p. 18, 2008.



Hindawi

Submit your manuscripts at
<http://www.hindawi.com>

